PHYSICAL REVIEW B VOLUME 60, NUMBER 16 15 OCTOBER 1999-II

Far-infrared gaps in single-wall carbon nanotubes

A. Ugawa, A. G. Rinzler, and D. B. Tanner
Department of Physics, University of Florida, Gainesville, Florida 32611-8440
(Received 17 June 1999)

The infrared properties of single-wall carbon nanotubes have been measured over 15–5000 cm^{-1}. The sample is a freestanding film composed of purified nanotubes. The temperature dependence of the reflectance is quite small at all temperatures studied (7.8 to 298 K) and no vibrational features are observed. The spectrum has a clear plasma edge, analyzed by a Drude model combined with a low-frequency localized absorption at 135 cm^{-1}. The absorption band is assigned to a pseudogap in armchair nanotubes and/or to very small gaps in zigzag or chiral nanotubes. [S0163-1829(99)50640-1]

Since their discovery by Iijima,[1] carbon nanotubes have been widely studied on account of their unique electronic[2–4] and mechanical[5,6] properties, properties which vary with the symmetry and environment of the tubes. Several workers have investigated the electronic structures of isolated single-wall nanotubes (SWNT's) as well as bundled nanoropes. For isolated tubes it is reported that (n,n) (armchair) SWNT's are metallic, whereas $(n,0)$ (zigzag) and (n,m) (chiral) tubes are semiconducting, most with a gap of 0.7 eV or so.[2,3,7] In certain cases ($n \equiv m$, mod 3) a very small band gap induced by the tube curvature is predicted.[2,7] It has also been theorized that nanoropes made from (n,n) nanotubes develop a pseudogap due to a broken symmetry caused by intertube coupling.[8] No optical data for low-energy regions has been reported up to now because of obvious difficulties in using long-wavelength light to measure microscale samples. Recently, a method to prepare free-standing SWNT films has been reported,[9] enabling the measurement of the infrared properties in the bulk state. In this contribution, we present the far-infrared reflectance of SWNT's, in which we show an evidence for far-infrared gaps in a bulk sample.

Laser-vaporization grown SWNT's (Ref. 10) were purified, made into a free-standing film, and characterized as described in Ref. 9. The film had a thickness of 20–40 μm, and showed no transmittance over the entire range of 15–5000 cm^{-1} (2–620 meV). The reflectance was measured on a Bruker IFS 113v using a reflectance unit and a liquid Helium flow cryostat. The sample was rigidly affixed to a specially designed, demountable sample holder which travels with the sample throughout all measurement/process steps (e.g., gold-coating) and permits repositioning of the sample, within the spectrometer cryostat, to an accuracy estimated to be as good as ± 10 μm. The cryostat/sample chamber space is small enough to permit rapid evacuation and sample exchange, without the need to vent and re-evacuate the entire spectrometer (a process which can lead to larger dimensional changes and spectral differences). The shift due to thermal contraction of the cryostat cold finger is compensated for by a remote-operated z stage, which can re-index the sample to its original height to within ± 2.5 μm accuracy.

Because of the roughness of the sample surface, we obtained the reflectance by normalizing a sample spectrum with the spectrum measured again at the same temperature after evaporating gold on the sample surface. The gold coating does not change the sample roughness appreciably, being less than 100 nm thick whereas the roughness observed in an optical microscope is on the order of 10 μm. This coating method to estimate the scattering loss in reflectivity on a rough surface works under the assumption that the scattering properties of the gold-coated surface are identical to the scattering properties of the nanotubes surface. This assumption has a defect that is possibly worse than the slight smoothing of the surface due to overcoating by the metal: because the dielectric functions are different, the scattering properties should also be different. However, the nanotubes are ''metallic'' and therefore ε is relatively large in magnitude, like gold, so the correction is a reasonable first-order procedure. We also note that the two defects mentioned above partially compensate: the rough gold surface is probably a stronger scatterer than the rough nanotube surface, but the gold coating slightly softens the roughness, diminishing the scattering.

The light source stability was monitored by measuring a gold reference mirror also located in the cryostat: this showed no significant change during the experiment period. The total experimental error is estimated to be within $\pm 0.5\%$ below 1000 cm^{-1}. We have checked the effect of shifting our reflectance up and down by the possible experimental error of 0.5% on our Kramers-Kronig results: the shifts only generated small quantitative effects in the optical conductivity. For the higher-frequency region, the reflected light becomes more diffuse due to the roughness of the sample surface, and the error increases to $\pm 2.5\%$ at 5000 cm^{-1}. However, the errors in this higher-frequency region did not qualitatively affect the far-infrared conductivity discussed later. We also investigated the temperature dependence of the film dc conductivity by a four-probe method to compare the dc results with the extrapolated optical conductivity.

Figure 1 shows the reflectance of the SWNT film measured at 298 K (top) and 7.8 K (bottom), with spectral resolutions of 4 cm^{-1} (500–5000 cm^{-1}), 2 cm^{-1} (80–500 cm^{-1}), and 1 cm^{-1} (15–80 cm^{-1}). The temperature dependence is quite small, and no vibrational structures are observed even at low temperatures, except for a small kink at 510 cm^{-1} [in contrast, graphite exhibits an in-plane stretching mode at 1589 cm^{-1} (Ref. 11)]. The spectra have a Drude-like appearance: the reflectivity monotonically decreases as photon energy increases, with a plasma edge around 2500 cm^{-1}. Measurements on samples from a second batch are qualitatively

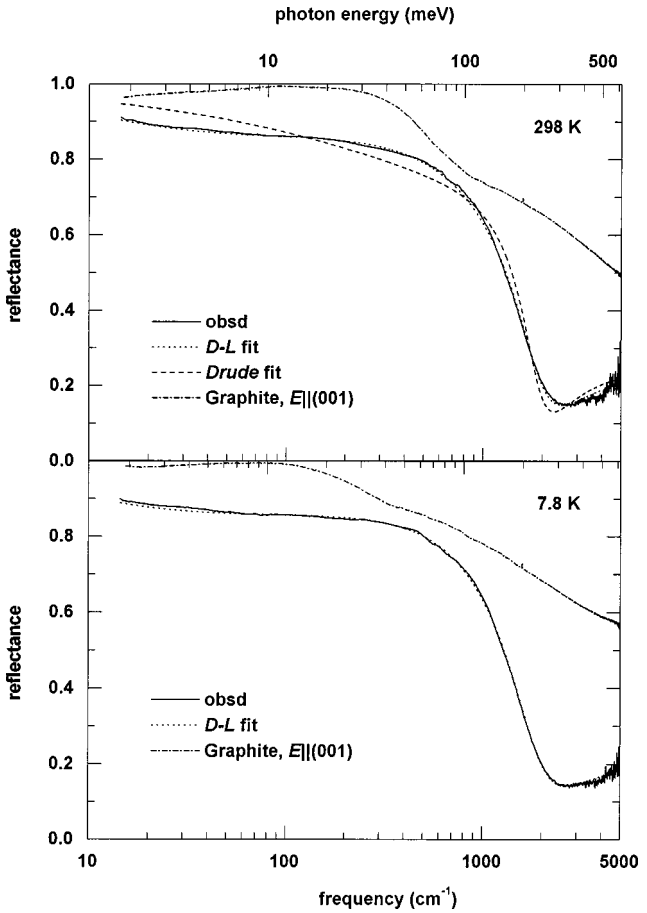

FIG. 1. Reflectance of SWNT's film measured at 298 K (top) and 7.8 K (bottom). The dotted line shows the simulated curves by the Drude-Lorentz model, and the dashed line is the best fit using only a Drude term (see text). The reflectance of graphite is also given in the dot-dashed line for comparison.

similar, with the plasma edge at the same frequency but with a somewhat higher far-infrared reflectance. The difference is attributed to a denser morphology in these samples.[12] The spectrum differs in important ways from graphite, which has its plasma edge at higher frequencies and a strong interband transition around 45 cm^{-1}.[13] The latter dominates in the far-infrared region, causing a reflectance peak around 100 cm^{-1}, which cloaks the contributions from intraband transitions.

The spectrum of the SWNT film, however, cannot be interpreted within the framework of a simple Drude model. We employ a model dielectric function, a combination of a Drude term and localized Lorentzian absorptions, given by[14]

$$\varepsilon(\omega)=\varepsilon_c-\frac{\omega_p^2}{\omega(i\gamma+\omega)}-\sum_j\frac{\Omega_{pj}^2}{(\omega^2-\omega_j^2)+i\Gamma_j\omega}, \quad (1)$$

where ε_c stands for the frequency-independent dielectric constant, ω_p and γ are, respectively, the plasma frequency and the relaxation rate of the charge carriers, and ω_j, Γ_j, Ω_{pj} are the center frequency, spectral width, and oscillator strength of the Lorentz oscillators for the localized transitions. The reflectance calculated with the parameters given in Table I is shown in both panels of Fig. 1 as a dotted line. Only a single localized absorption was needed to obtain complete agreement with the measurement. The upper panel

TABLE I. Analysis of the reflectance by the Drude-Lorentz model.

	ε_c	ω_p (eV)	γ (eV)	Ω_{pj} (eV)	ω_j (eV)	Γ_j (eV)
298 K	8.5	0.64	0.25	0.45	0.020	0.042
7.8 K	7.6	0.65	0.36	0.47	0.021	0.041

of Fig. 1 also shows the best fit obtained using only a Drude term of Eq. (1) in a dashed line: in this case the fit apparently describes the data poorly. The localized band has about 33% of the total low-energy spectral weight, and should thus come from intrinsic properties of the sample, not from extrinsic features such as impurities. The fitting parameters are almost the same between 298 and 7.8 K, except that the relaxation rate γ is significantly larger at low temperature. The zero-frequency conductivity, given by $\sigma(0)=\varepsilon_0\omega_p^2/\gamma$, is calculated to be 220 S cm^{-1} at 298 K and 160 S cm^{-1} at 7.8 K. This nonmetallic behavior is consistent with the semiconducting transport properties of this film, as discussed later.

In Fig. 2 (top) we show the real part of the conductivity (σ_1) obtained by a Kramers-Kronig transformation of the reflectance. The dielectric functions from an electron energy-loss (EELS) experiment[15] were used to extrapolate our reflectance to high frequencies and the curve fitting results given in Table I were applied at low frequencies. The con-

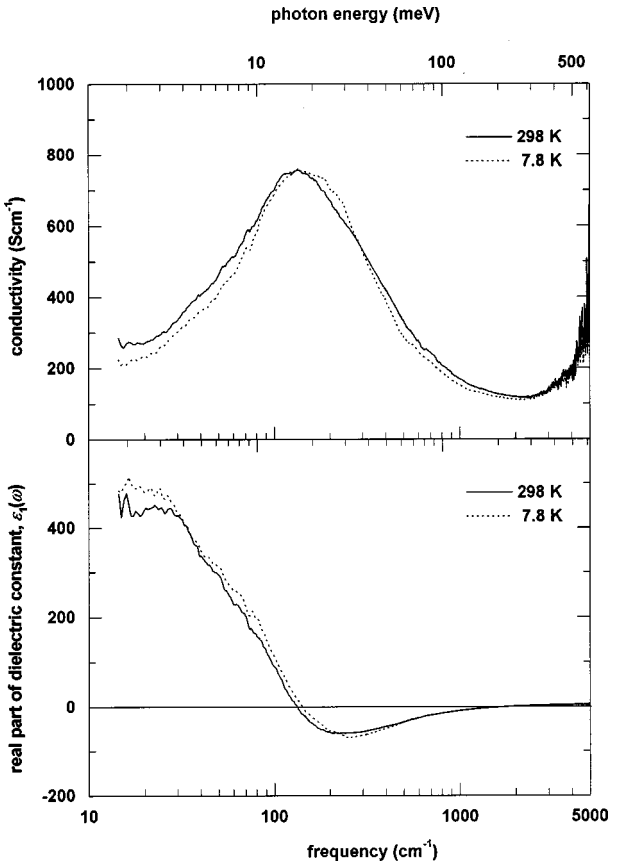

FIG. 2. Real parts of the conductivity $[\sigma_1(\omega)]$ (top) and dielectric function $[\varepsilon_1(\omega)]$ (bottom) of SWNT's film obtained by a Kramers-Kronig analysis of the reflectance.

ductivity shows a strong peak at 135 cm^{-1} (17 meV), corresponding to the Lorentzian absorption mentioned in the previous paragraph. The temperature dependence is very small as well as that of the reflectance. The extrapolated dc conductivity is estimated to be 200 $S\,cm^{-1}$ at 298 K and 150 $S\,cm^{-1}$ at 7.8 K, in good agreement with what is estimated from the fit to Eq. (1). The localized absorption dominates the spectra, despite its smaller weight in the fit above. The contribution of free carriers is not predominant anywhere in the measured spectral range. This conclusion is evident from the real part of dielectric function, $\varepsilon_1(\omega)$, shown in Fig. 2 (bottom). A free-carrier response is characterized by large negative values of $\varepsilon_1(\omega)$ with decreasing photon energy in the infrared.[16] The ε_1 of the SWNT film becomes negative below 1680 cm^{-1}, but turns positive again around 145 cm^{-1} to exhibit a dielectric character in the low-frequency region. This feature no doubt originates from the localized band at 135 cm^{-1} in the conductivity.

We also measured the resistivity of the SWNT film, using pieces from the samples employed in the reflectance measurements. The absolute resistivity at 298 K was 10–20 $m\Omega\,cm$, more than twice the optically estimated value. Note that we made no correction to this observed dc resistivity for the density, as has been done in the other reports.[9,17] The temperature dependence was semiconducting in character: the ratio $\rho(7.8\,K)/\rho(298\,K)\sim 5$ compared to 1.3 for the optical results. This temperature dependence is close to that observed for nanoropes with tangled regions,[17] consistent with the film structure, where a huge number of nanoropes are bundled and/or tangled so as to make a bulk film.

We now discuss the interpretation of the far-infrared optical conductivity of the SWNT film. The electronic structure of individual SWNT is specified by a pair of integers (n,m), which represent a coordinate of the wrapping vector in the hexagonal lattice of graphite single sheet.[3] Hamada *et al.* used tight-binding band calculations to predict that achiral, armchair SWNT's of $n=m$ are gapless and should be metallic, while zigzag or chiral SWNT's of $n\neq m$ have a gap that varies depending on the wrapping vector.[2] These features were theoretically explained by Kane and Mele as follows: most of these SWNT's have a primary gap (scaling as $1/R$, where R is a tube radius) on the order of 1 eV, but in one case of $n\equiv m$ (mod 3) this gap completely vanishes; there is, however, still a very small gap on the order of 10 meV induced by the tube curvature scaling as $1/R^2$; this secondary gap vanishes only when $n=m$ armchair structures.[7] In the case of (n,n) SWNT's organized into bundles or ropes, moreover, Delaney *et al.* argued, using an empirical pseudopotential method, that the intertube couplings cause a broken symmetry of the tube, inducing a pseudogap at the Fermi level.[8] Either or both of these effects could be reasonable for the far-infrared gaplike feature in our spectra.

The modest temperature dependence and the persistence of the gap to room temperature seen in the reflectance result may seem unusual. We note, however, that graphite has an electronic gaplike feature at 45 cm^{-1} at room temperature, even lower than in the SWNT film, which is similarly weakly temperature dependent. Moreover, unlike a semiconductor, the density of mobile carriers in the nanotube film is large even at low temperatures. Furthermore, the gap here is caused by *symmetry* and hence is not as vulnerable to temperature as a charge density wave (CDW) or superconducting gap.

The optically estimated dc conductivity is much smaller than that reported on an isolated rope of SWNT's, and this property must originates from the heterogeneous nature of our film sample, complicating the interpretation of the data shown here. Some experiments have reported that SWNT's prepared in this manner have up to 40% (10,10) tubes[18] while others have suggested that no one species dominates.[19,20] Even in the former case, our sample is a composite consisting of a random mixture of tubes of different types, oriented rather randomly at least within the plane of the film, and a considerable density of voids. Here we take two approaches to our analysis. First, we evaluate the spectral weight originated from metallic or small-gap SWNT's in the low-energy region ($\omega<4000$ cm^{-1}) and compare that with the spectral weight observed in higher-energy transitions ($4000\,cm^{-1}<\omega<8000\,cm^{-1}$) where only semiconducting SWNT's can contribute.[2,7,19] This comparison tells us the fraction of the tubes that have metallic or small band gap character. Second, we perform an effective medium calculation for the optical conductivity of an assumed two-constituent mixture of metallic and semiconducting components and compare that to the Kramers-Kronig derived conductivity.

The effective number of carriers $N_{\rm eff}$ participating in optical transitions at frequencies less than ω is given by

$$N_{\rm eff}(\omega)\,\frac{m}{m^*}=\frac{2mV_{\rm cell}}{\pi e^2}\int_0^{\omega}\sigma_1(\omega')\,d\omega', \qquad (2)$$

where e and m are the free-electron charge and mass, respectively, m^* is the effective mass, and $V_{\rm cell}$ is the volume occupied by one formula unit. For the latter, we take the volume of 40 carbons, i.e., the volume of a single turn of a (10,10) nanotube, being 600 $Å^3$. We performed the numerical integrals and found $N_{\rm eff}(4000\ cm^{-1})\sim 0.2$ and $N_{\rm eff}(8000\ cm^{-1})\sim 0.6$. This results in a ratio of 1:2 for the amount of

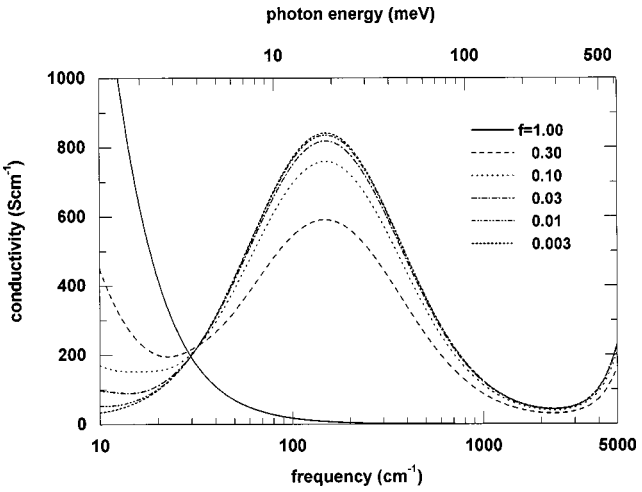

FIG. 3. Calculated optical conductivities $[\sigma_1(\omega)]$ in the mixture of metallic and semiconducting SWNT's using an effective medium approximation (EMA). The curves are shown for metal SWNT fractions of 1.00 (solid), 0.30 (dashed), 0.10 (dotted), 0.03 (dash-dotted), 0.01 (dash-dot-dotted), and 0.003 (short-dashed).

metallic or small-gap SWNT's to semiconducting SWNT's in our film. This value is reasonable if SWNT's were generated randomly, because one third of the SWNT's should belong to a metallic or small-gap class under the $n \equiv m \pmod 3$ condition.

The effective dielectric function for the mixture of needle-shaped metallic and semiconducting nanotubes can be expressed by the effective medium approximation (EMA) (Ref. 21) as the solution (with positive imaginary part) to

$$f\frac{\varepsilon_m-\varepsilon}{g\varepsilon_m+(1-g)\varepsilon}+(1-f)\frac{\varepsilon_g-\varepsilon}{g\varepsilon_s+(1-g)\varepsilon}=0, \qquad (3)$$

where f is the volume fraction of metallic tubes with ε_m, $1-f$ is the volume fraction of semiconducting tubes with ε_s, and g is the depolarization factor. We take $g=0.01$ for needle-shaped SWNT's and use for the metallic tubes the Drude term of the graphite reflectance shown in Fig. 1.[22] For the semiconducting tubes, the parameters are based on the Lorentzian parts of the curve-fitting result on the film reflectance.[22] The optical conductivity curves calculated for several concentrations f are given in Fig. 3. In concentrations between 10 and 30%, the calculations closely resemble the measured conductivity in Fig. 2. One might expect that the far-infrared absorption is due to a small-particle resonance caused by diluting metallic nanotubes with semiconducting nanotubes. We have also performed the EMA calculations without the far-infrared absorption band from the parameter set used above. The result is a very weak absorption (less than 10 S cm^{-1} at the peak in the conductivity) around 200 cm^{-1}. We therefore conclude that the far-infrared band is essential to the sample constituent, nanotubes and nanoropes.

The low-energy absorption band observed in the optical conductivity at 135 cm^{-1} (17 meV) could arise from two courses: (i) the pseudogap in bundled (n,n) SWNT's although its value is less than a half of the predicted value for (10,10) SWNT's; (ii) the secondary gaps (5–20 meV) calculated for small-gap SWNT's with 13–15 Å diameters.[7] Indeed, the observed far-infrared band could be due to an average of these two kinds of transitions.

This work was supported by the National Science Foundation through Grant No. DMR-9705108.

[1] S. Iijima, Nature (London) **354**, 56 (1991).
[2] N. Hamada, S. Sawada, and A. Oshiyama, Phys. Rev. Lett. **68**, 1578 (1992).
[3] R. Saito *et al.*, Appl. Phys. Lett. **60**, 2204 (1992).
[4] S. J. Tans *et al.*, Nature (London) **386**, 474 (1997).
[5] E. W. Wong, P. E. Sheehan, and C. M. Lieber, Science **277**, 1971 (1997).
[6] M. B. Nardelli, B. I. Yakobson, and J. Bernhole, Phys. Rev. B **57**, R4277 (1998).
[7] C. L. Kane and E. J. Mele, Phys. Rev. Lett. **78**, 1932 (1997).
[8] P. Delaney *et al.*, Nature (London) **391**, 466 (1998).
[9] A. G. Rinzler *et al.*, Appl. Phys. A: Mater. Sci. Process. **67A**, 29 (1998).
[10] A. Thess *et al.*, Science **273**, 483 (1996).
[11] R. J. Nemanich, G. Lucovsky, and S. A. Solin, Solid State Commun. **23**, 117 (1977).
[12] A. Ugawa, A. G. Rinzler, and D. B. Tanner (unpublished).
[13] Y. Sato, J. Phys. Soc. Jpn. **24**, 489 (1968); H. Philipp, Phys. Rev. B **16**, 2896 (1977).
[14] A. Ugawa *et al.*, Phys. Rev. B **38**, 5122 (1988).
[15] T. Pichler *et al.*, Phys. Rev. Lett. **80**, 4729 (1998).
[16] L. G. Schulz, Philos. Mag. Suppl. **6**, 102 (1957).
[17] J. E. Fischer *et al.*, Phys. Rev. B **55**, R4921 (1997).
[18] J. M. Cowley *et al.*, Chem. Phys. Lett. **265**, 379 (1997).
[19] J. W. G. Wildöer *et al.*, Nature (London) **391**, 59 (1998).
[20] T. W. Odom *et al.*, Nature (London) **391**, 62 (1998).
[21] R. Landauer, J. Appl. Phys. **23**, 779 (1952); in *Electrical Transport and Optical Properties of Inhomogenous Media*, edited by J. C. Garland and D. B. Tanner (AIP, New York, 1978).
[22] The employed parameters for EMA calculations are as follows. The graphite Drude term: $\omega_p=1520$ cm^{-1} and $\gamma=4.6$ cm^{-1} (this set is consistent with the observed dc conductivity of individual ropes (Ref. 17); the semiconducting SWNT terms: $\Omega_{p1}=4500$ cm^{-1}, $\omega_1=150$ cm^{-1}, $\Gamma_1=400$ cm^{-1}, $\Omega_{p2}=7500$ cm^{-1}, $\omega_2=6000$ cm^{-1}, $\Gamma_2=3000$ cm^{-1}, and $\varepsilon_c=4.9$.